Zeitschrift: IABSE publications = Mémoires AIPC = IVBH Abhandlungen
Band: 27 (1967)

Artikel: Prestressed suspended roofs bounded by main cables
Autor: Siev, Avinadav
DOI: https://doi.org/10.5169/seals-21548

Nutzungsbedingungen
Die ETH-Bibliothek ist die Anbieterin der digitalisierten Zeitschriften auf E-Periodica. Sie besitzt keine Urheberrechte an den Zeitschriften und ist nicht verantwortlich für deren Inhalte. Die Rechte liegen in der Regel bei den Herausgebern beziehungsweise den externen Rechteinhabern. Das Veröffentlichen von Bildern in Print- und Online-Publikationen sowie auf Social Media-Kanälen oder Webseiten ist nur mit vorheriger Genehmigung der Rechteinhaber erlaubt. Mehr erfahren

Conditions d'utilisation
L'ETH Library est le fournisseur des revues numérisées. Elle ne détient aucun droit d'auteur sur les revues et n'est pas responsable de leur contenu. En règle générale, les droits sont détenus par les éditeurs ou les détenteurs de droits externes. La reproduction d'images dans des publications imprimées ou en ligne ainsi que sur des canaux de médias sociaux ou des sites web n'est autorisée qu'avec l'accord préalable des détenteurs des droits. En savoir plus

Terms of use
The ETH Library is the provider of the digitised journals. It does not own any copyrights to the journals and is not responsible for their content. The rights usually lie with the publishers or the external rights holders. Publishing images in print and online publications, as well as on social media channels or websites, is only permitted with the prior consent of the rights holders. Find out more

Download PDF: 08.01.2026

ETH-Bibliothek Zürich, E-Periodica, https://www.e-periodica.ch

Prestressed Suspended Roofs Bounded by Main Cables

Couvertures précontraintes suspendues limitées par des câbles principaux

Vorgespanntes Hängedach mit Randkabel

AVINADAV SIEV
New-York, USA

Introduction

Several studies [1, 2, 3, 4] have recently been published on the analysis of two-directional prestressed cable nets under the following limitations:

a) The cables in each direction lie in parallel vertical planes, with the two sets of planes usually perpendicular to each other.
b) The frame bounding the net is stiff, i. e. its deformation is negligible.

In ref. [3, 6], a method is described by which frame deformation may be taken into account by the following iterative procedure: the joints at the boundary assumed as fixed and the net is solved; variation of the forces acting on the boundary joints is then calculated, yielding the frame deformation; the effect of the latter on the net is finally determined, and iteration is carried on to the desired degree of accuracy. A general theory for prestressed suspended nets, published recently [4], permits solution of any type of net under any boundary conditions, with non-linearity taken into account.

The present paper is an analytical and experimental study of one of the simplest models of suspended roof bounded by main cables (Fig. 1). The model consists of four main cables 12-13, 13-14, 14-15, 15-12, fixed at points 12, 13, 14, 15. Two of the fixing points 12 and 14 are elevated, and the other two depressed. Four diagonals are stretched in each direction between the main cables. The model approximates a hypar surface bounded by parabolas in plan (Fig. 2). When a denser net is used, cables 2-5 and 6-9 tend to a convex parabola and cables 0-11 and 1-10 to a concave one. It is easily proved that a system of this shape, composed of bars with frictionless ball joints, is unstable [6]. For a determinate structure the number of bars should be $3J$, where J is the number

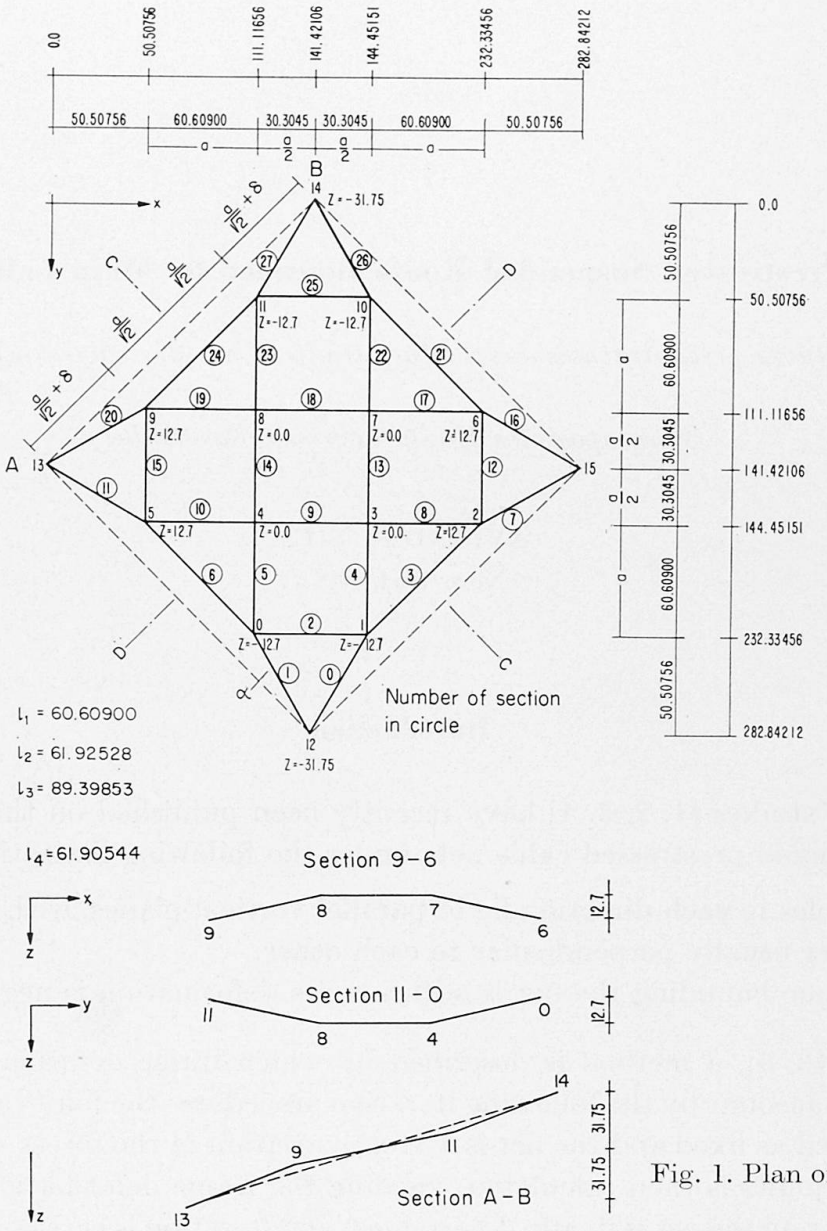

Fig. 1. Plan of the model.

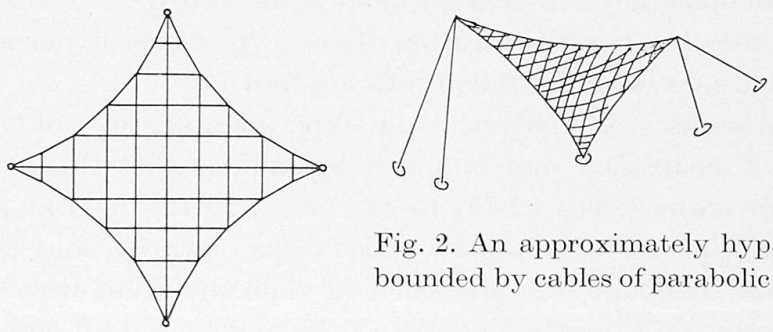

Fig. 2. An approximately hypar surface net bounded by cables of parabolic shape in plan.

of inner joints. In this case $J = 12$, but there are only 28 bars instead of the 36 necessary for a determinate system. In the case of prestressed cables, however, a certain degree of stabilization is provided, as shown for similar suspended roofs [3]. The higher the prestress, the stabler the system.

The object of the present study was analysis of the behaviour of a system of this type under various modes of loading, checking the effectiveness of the theory by means of the model, and comparison of numerical and experimental results. The theory, once verified, permits any real structure to be solved directly without recourse to similarity considerations.

The Model

Fig. 3 is a photograph of the model. A frame with a smaller cross section would have sufficed from the statical point of view, but excessive dimensions were used so as to obtain extremely high stiffness and minimum deflections. Joints 12, 13, 14, 15 were anchored to a welded frame of 4″ ∅ pipes. The spacing of the anchorage points was 200 × 200 cm and the height — 63.5 cm.

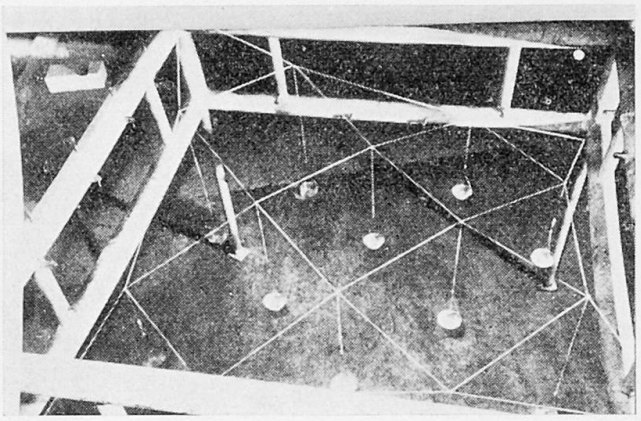

Fig. 3. A picture of the model.

The horizontal component (H) of tension in all diagonal cables was assumed constant and different from its tensile counterpart (H_1) in the center of the main cable (sections 3, 6, 21, 24). It was also assumed $\tan\alpha = 0.25$ (α angle in the horizontal plane, as defined in Fig. 1), hence $a = 60.609$ cm; $\delta = 14.286$. All other dimensions and coordinates are given in Fig. 1. For equilibrium in the horizontal plane, we must have

$$H_1 = \frac{\sqrt{2}}{\delta}\left(\frac{a}{\sqrt{2}} + \delta\right) H. \tag{1}$$

Points 3, 4, 7, 8 are at mid-height; 1 and 2 are symmetrical with respect to mid-height. In other words, an equilibrium equation of the vertical prestress components forces in the unloaded system contains a single unknown — the elevation $\pm f$ of points 0, 1, 2, 5, 6, 9, 10, 11, namely:

$$\frac{H}{a} f + \frac{2 H_1}{a\sqrt{2}} f - \frac{H_1}{\frac{a}{\sqrt{2}} + \delta}\left(\frac{63.5}{2} - f\right) = 0. \tag{2}$$

On substituting H_1 from Eq. (1), H is eliminated, implying that it is irrele-

vant to the shape. Rearranging and simplifying, we obtain:

$$f = \frac{63.5}{\sqrt{2}} \frac{a}{3\,\delta + 2\sqrt{2}\,a} \tag{3}$$

or:

$$f = 12.7 \text{ cm}.$$

The exact length of each section is now obtainable with the aid of Pythagoras' theorem.

As the cables are prestressed, their initial length should be less than the geometrical length l of the section.

$$l = l_0 \left(1 + \frac{T}{E\,A}\right). \tag{4}$$

The model was formed from three wires (Fig. 4): One (representing the main cable) 1 mm in diameter, and the other two 0.5 mm. Each wire formed a loop with a single joint, cut to its exact length with the smallest possible tolerances (say below 1 mm). The length of each section was marked consecutively on the

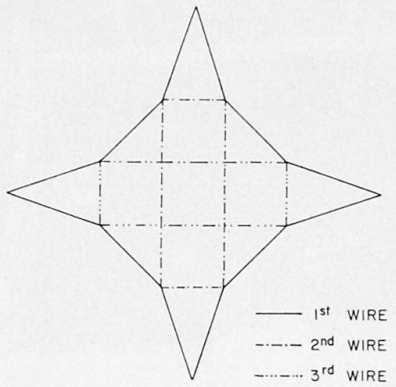

Fig. 4. The tree wires forming the model.

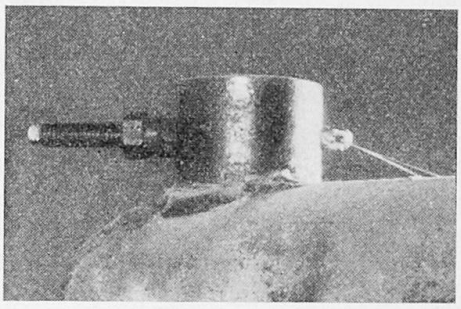

Fig. 5. Anchorage of the model.

wires, and connections at the joints were formed by soldering. Vertical wires were connected to each joint, from which scales were suspended for holding load weights. Prestressing was applied by screws (Fig. 5) at all anchorage joints, permitting some correction of inaccuracies in wire length. Tension in the wires was measured by a dynamometer, described on an earlier occasion [3]. Comparison of tension in the sections (which should theoretically be equal), indicates the degree of accuracy in the erection of the model. The tension in the wires was determined as 4.15 kg ± 0.150 kg, i. e. tolerances of ± 3.5%. The modulus of elasticity was 1.9×10^6 kg/cm² for the 0.5 mm ⌀ wires and 1.95×10^6 kg/cm² for the 1.0 mm ⌀ wire.

Symmetry of Model

The model is symmetrical about two diagonal axes, and antisymmetrical about axes C-C and D-D. Considering single concentrated loads, a load at 0 is

identical to one at 1 as to its effect on symmetrical joints, hence the deflection of joints 0 will be the same as that of joint 1. Horizontal displacement to the right (positive) under a concentrated load on 0 will correspond to one of the same magnitude to the left (negative) under a load on 1. This will not be the case for joints 1 and 2 owing to the non-linearity of the structure, but if non-linearity is neglected under small loads these two joints will also be identical. As the deflection versus load curves are non-linear, deflections under a positive load P_1 are not necessarily equal (in absolute value) to those under an equal negative load. On reversing the model, the lower joints (2, 5, 9, 6) will become the upper ones and vice versa, with the load at 1 directed upwards; as the effect of a negative load is not equal to that of a positive one, joints 1 and 2 will not behave identically. Actually, only three cases need be considered, namely those of joints 1, 2 and 3 under positive load, and the effect of negative concentrated load may be deduced from the above information. For example, the deflection of 1 due to negative load at 1 is equal to minus the deflection of 2 under the same positive load at 2; on the other hand, the deflection of 3 under a load at 3 is antisymmetric for positive and negative loads. More symmetry features will be discussed later.

Experimental

Weights representing single concentrated loads were applied to all joints in 200-gram increments from zero to 2000 grams. All corresponding vertical deflections were measured as a check of accuracy, and averages were used for comparison with theoretical results [7].

Measurement Technique

In earlier tests on nets of different form [3], curves plotted on the basis of deflectometer readings were not smooth, probably due to friction. An optical level Wild N 3 type was used accordingly in the present study. Deflectometer accuracy is 1/100 mm as against 1/10 mm for a level (although 3/100 is obtainable by interpolation). The loss of accuracy was offset by elimination of friction and of any other external interference with the system. In the event, the choice justified itself. No convenient means was found for measuring the horizontal components, but in view of the satisfactory correspondence observed in the vertical components, the same may be assumed with regard to the former.

Method of Computation

The general theory [4] was chosen for solving the system. Although involving a larger number of equations than other theories [6], it was considered the sim-

Table 1. Comparison of measured and computed deflections U

Load kg	Measured $U_{3,0;0}$		Measured $U_{3,1;1}$		Measured $U_{3,10;10}$		Measured $U_{3,11;11}$		Average measured	U Computed	U Corrected*)
	Load	Unload	Load	Unload	Load	Unload	Load	Unload			
0.0	0.000	0.001	0.000	–0.001	0.000	–0.003	0.000	0.001	0.000	0.000	0.000
0.2	0.203	0.204	0.202	0.203	0.198	0.196	0.196	0.198	0.200	0.213	0.197
0.4	0.390	0.395	0.402	0.399	0.389	0.379	0.393	0.393	0.393	0.432	0.393
0.6	0.591	0.591	0.605	0.601	0.580	0.577	0.592	0.592	0.592	0.630	0.586
0.8	0.789	0.791	0.792	0.797	0.767	0.765	0.795	0.782	0.784	0.833	0.775
1.0	0.978	0.978	0.991	0.995	0.959	0.957	0.963	0.963	0.973	1.032	0.960
1.2	1.170	1.171	1.183	1.184	1.141	1.142	1.157	1.159	1.163	1.224	1.141
1.4	1.359	1.357	1.379	1.370	1.322	1.321	1.344	1.344	1.348	1.411	1.317
1.6	1.545	1.537	1.556	1.550	1.506	1.503	1.526	1.523	1.530	1.593	1.489
1.8	1.725	1.723	1.744	1.741	1.679	1.683	1.706	1.707	1.713	1.768	1.655
2.0	1.905	1.905	1.929	1.929	1.862	1.862	1.884	1.884	1.895	1.937	1.816

*) Corrected computed values — those obtained after increasing EA by 6% and T by 8%. In this case, the correction changed the discrepancy between computed and average measured results from about $+2\%$ to about -4%.

(Note: The first subscript refers to direction, i. e. X_3 or Z axis; the second to the point of force application; the third to the observed point.)

plest and most promising method. The system contains 16 joints, of which 4 are fixed anchorage joints and 12 are inner joints. The unknowns are the three components of displacement of each inner joint, i. e. a total of 36. A program was prepared for the Philco 2000 computer, which yielded the matrix terms, the new coordinates of each joint, the elongation of the wire sections and the new tension in each. Finnally, the residual force at each joit was determined, and wherever it exceeded 0.1 gram, the calculation was repeated, using the new coordinates and with the residuals as loads. Each cycle was continued until all residuals were less than 0.1 gram, when loads were increased or the point of application changed and the same procedure was re-applied. It should be noted that each cycle required about 4.4 seconds, including iterations.

Experiment vs. Theory

Test results show excellent agreement between deflections which should be equal. The deflections of points 0, 1, 10, 11 due to loads at the same points are given in Table 1. It is seen that the difference between deflections on loading and unloading are of the order of measurement accuracy. There was no hysteresis, and on complete unloading, the system resumed its initial shape. The difference between deflections is so small, that all 8 graphs would practically coincide. The same situation was encountered in all other deflections and justifies complete confidence in the test technique. Computed results showed larger deflections than the measured ones. The difference in percentage was smaller for the large deflections and larger for the small deflections. Except where deflections are negligible (i. e. of the order of accuracy) discrepancies between experiment and theory ranged from 2% to 30% (mostly 2—10%), and although such error may be permissible, steps were taken to reduce it, as will be explained later.

Sources of Error

The sources of error may be summarized as:

a) Inaccuracy in determining the prestress force T and the rigidities EA.
b) Inaccuracy in system geometry.
c) Neglected joint rigidity due to soldering, and bending rigidity of the wires.
d) Yielding of anchorage joints due to deflections in the ∅ 4″ pipe frame.
e) Inaccuracy in the assumed ratio of T or EA between the small (0.5 mm) and larger diameter wire (1.0 mm).
f) Inaccuracy of the theory.

It is improbable that temperature changes should be a source of error, since the tests were carried out in a closed hall where both frame and wires

should be equally affected. Moreover, such a factor should be reflected in the comparison of theoretically equal deflections. The negligible scatter in the results rules out source b). Source f) is similarly unlikely, since the theory is based on the first principles of equilibrium, the only assumption being absence of flexural stiffness in the wires, i. e. they are moment free, and that the system is weightless.

The likeliest sources are a) and e).

The method of determining the tension and rigidities could easily introduce an error of several percent. The effect of the soldering on rigidity is also uncertain.

Reducing the Discrepancy

In order to reduce the number of combinations, it was decided to disregard source e) and examine the effect of varying T and EA. This was done by increasing each parameter by 2.5% increments and computing all deflections under 2.0 kg for each of the combinations. Using a slightly modified computer program, a diagram as in Fig. 6 was plotted for each of the vertical deflections. Thus, for the original assumption the deflection was 0.614 cm, while for an increase of 5% in EA and 2.5% in T. The deflection is 0.60 cm. For small loads the principal effect was due to variation of tension, while that of rigidity was small; for higher loads the picture is reversed. Isopleths of equal deflections were traced and transferred to Fig. 7. Had the discrepancy been solely due to errors in EA and T, all isopleths would have been concurrent, and their common point of intersection would determine the correction percentage; this was not the case, but most lines indicated an increase of 8% in T and 6% in EA. (See Table 2 and Fig. 8.)

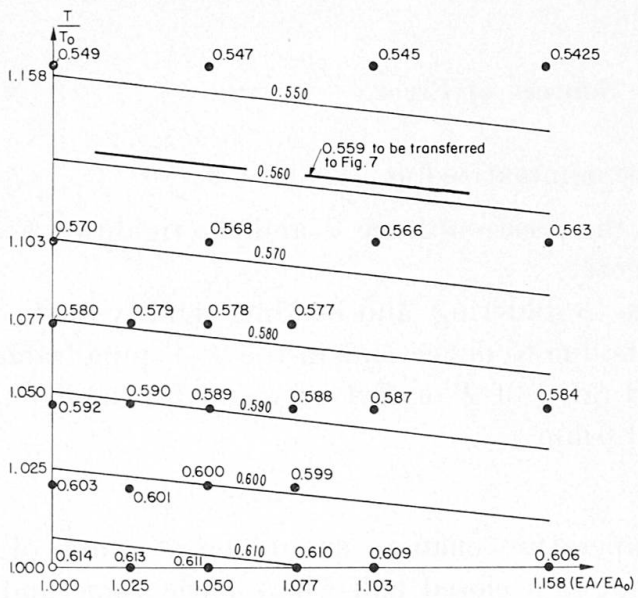

Fig. 6. Lines of equal deflections as a function of EA and T.

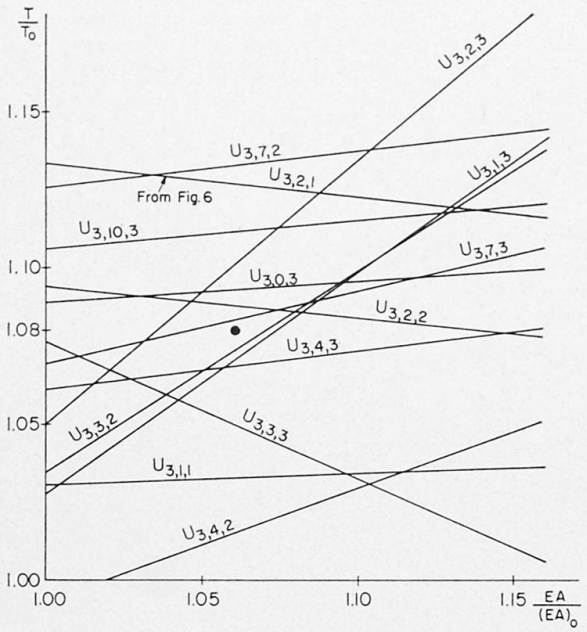

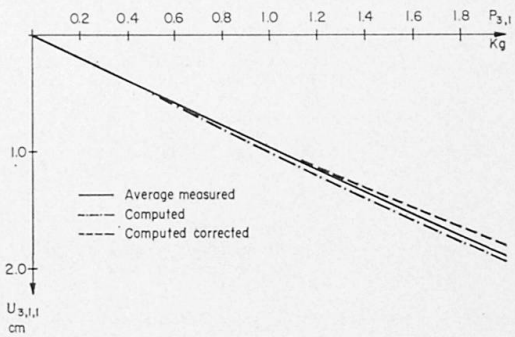

Fig. 8. Comparison of computed and calculated results.

Fig. 7. Lines of the deflections as a function of T and A.

Table 2. Differences between measured and computed deflections

$P = 2.0$ kg, $EA = 1.06\, EA_0$, $T = 1.08\, T_0$

No. of cases	Percentage difference	Average of absolute value of deflection in cm
17	0— 5	0.61
6	5—10	0.25
6	10—35	0.14
7	Deflections too small to be measured	0.02

Supplementary Computations

With the program ready and debugged, it seemed worthwhile to study the behaviour under higher concentrated single loads, as well as under equal vertical and equal horizontal loads at all joints. The original series comprised concentrated loads of 0 to 10 kg at 1 kg increments but, due to an error in the program, the case of a concentrated load at 1, up to 90 kg was also computed. Results were found of interest, and part of them is presented. The stresses in some of the wires were above ultimate strength, but the impracticability of the pattern is disregarded and certain curious features of non-linear behaviour of a structure of this kind are pointed out.

In the case of the load at point 3, calculations showed negative tension (i. e. compression) in two wires. As the wires are only capable of resisting tension, the program was modified, converting compression into zero and iterations

	0	1	2	3	4	5	6	7	8	9	10	11	12	13	14	15
X	111.2	171.8	232.4	171.8	111.2	50.6	232.4	171.8	111.2	50.6	171.8	111.2	141.4	0.0	141.4	282.8
Y	232.3	232.3	171.7	171.7	171.7	171.7	111.1	111.1	111.1	111.1	50.5	50.5	282.8	141.4	0.0	141.4
Z	-12.64	-12.76	12.57	-0.10	0.11	12.82	12.57	-0.10	0.11	12.82	-12.76	-12.64	-31.75	31.75	-31.75	31.75
PX	0.20	0.20	0.20	0.20	0.20	0.20	0.20	0.20	0.20	0.20	0.20	0.20				
PY	0.00	0.00	0.00	0.00	0.00	0.00	0.00	0.00	0.00	0.00	0.00	0.00				
PZ	0.00	0.00	0.00	0.00	0.00	0.00	0.00	0.00	0.00	0.00	0.00	0.00				

	0	1	2	3	4	5	6	7	8	9	10	11
UX	0.0404	0.0402	0.0549	0.0528	0.0530	0.0526	0.0549	0.0528	0.0530	0.0526	0.0402	0.0404
UY	-0.0079	0.0063	-0.0003	-0.0009	0.0010	0.0002	0.0003	0.0009	-0.0010	-0.0002	-0.0063	0.0079
UZ	0.0553	-0.0594	-0.1293	-0.1035	0.1084	0.1237	-0.1293	-0.1035	0.1084	0.1237	-0.0594	0.0553

SECTION	LENGTH (L)	TENSION (T)
0	61.902	24.504
1	61.909	26.358
2	60.609	4.145
3	89.393	23.529
4	61.923	4.123
5	61.927	4.369
6	89.404	25.423
7	61.900	24.190
8	61.922	4.046
9	60.609	4.159
10	61.929	4.453
11	61.910	26.681
12	60.608	4.112
13	60.607	4.036
14	60.611	4.275
15	60.609	4.172
16	61.900	24.190
17	61.922	4.046
18	60.609	4.159
19	61.929	4.453
20	61.910	26.681
21	89.393	23.529
22	61.923	4.123
23	61.927	4.369
24	89.404	25.423
25	60.609	4.145
26	61.902	24.504
27	61.909	26.358

```
TVB PX1 2140  FLOAT  0,1,1,1,1,1,1,1,1,1,1,1,1$
              JMP    13100
```

Fig. 9. A computer sheet for $P_x = 0.2$ kg at all joints (horizontal load in the x direction).

as before. Incidentally, it was found that 5 kg increments did not save time, as convergence was slow.

Additional computations were carried out for horizontal loads of 0.2 kg and 1.0 kg on all joints in the x-direction. Fig. 9 and Fig. 10 are photographs of the output sheets from the computer. The first 3 rows show the coordinates of the joints after deformation, and the next three — the loads. Joints 12, 13, 14 and 15 are fixed anchorages unaffected by load. Next come the three components of the deflections. The two lowermost give the length and tension for each section.

The same procedure was applied for vertical loas at all points.

Pin checks were carried to varify the computations. With coordinates and section lengths available, the direction cosines and equilibrium in each direction were calculated on a desk calculator. An additional check was effected by running a set of calculations for negative loads and comparing symmetrical and antisymmetrical results.

Non-linear Behaviour of the System

Part of the results, representing the most interesting features of the structure, are reported below:

	0	1	2	3	4	5	6	7	8	9	10	11	12	13	14	15
X	111.3	171.9	232.6	172.0	111.4	50.8	232.6	172.0	111.4	50.8	171.9	111.3	141.4	0.0	141.4	282.8
Y	232.3	232.3	171.7	171.7	171.7	171.7	111.1	111.1	111.1	111.1	50.5	50.6	282.8	141.4	0.0	141.4
Z	-12.45	-13.04	11.98	-0.46	0.58	13.27	11.98	-0.46	0.58	13.27	-13.04	-12.45	-31.75	31.75	-31.75	31.75
PX	1.00	1.00	1.00	1.00	1.00	1.00	1.00	1.00	1.00	1.00	1.00	1.00				
PY	0.00	0.00	0.00	0.00	0.00	0.00	0.00	0.00	0.00	0.00	0.00	0.00				
PZ	0.00	0.00	0.00	0.00	0.00	0.00	0.00	0.00	0.00	0.00	0.00	0.00				

	0	1	2	3	4	5	6	7	8	9	10	11
UX	0.2037	0.2007	0.3035	0.2631	0.2679	0.2428	0.3035	0.2631	0.2679	0.2428	0.2007	0.2037
UY	-0.0513	0.0153	-0.0019	-0.0033	0.0061	0.0004	0.0019	0.0033	-0.0061	-0.0004	-0.0153	0.0513
UZ	0.2503	-0.3375	-0.7174	-0.4608	0.5823	0.5664	-0.7174	-0.4608	0.5823	0.5664	-0.3375	0.2503

SECTION	LENGTH (L)	TENSION (T)
0	61.889	21.254
1	61.925	30.383
2	60.609	4.140
3	89.373	20.039
4	61.918	3.822
5	61.938	5.013
6	89.427	29.401
7	61.883	19.755
8	61.913	3.485
9	60.613	4.411
10	61.947	5.522
11	61.932	32.118
12	60.605	3.920
13	60.602	3.743
14	60.621	4.900
15	60.610	4.194
16	61.883	19.755
17	61.913	3.485
18	60.613	4.411
19	61.947	5.522
20	61.932	32.118
21	89.373	20.039
22	61.918	3.822
23	61.938	5.013
24	89.427	29.401
25	60.609	4.140
26	61.889	21.254
27	61.925	30.383

```
        JMP     2

**ERR DMP
**"ENDJOB
         SAME JOB 2
** SAME JOB     2
```

Fig. 10. A computer sheet for $P_x = 1.0$ kg at all joints.

Loading of Joint 1

Fig. 11 shows the vertical deflection of joint 1 — $U_{3,1,1}$ due to a vertical load on it ($P_{3,1}$) in the range -10 kg to $+90$ kg[1]).

The same may also represent the deflection of point 2 in the range -90 kg to $+10$ kg. The curve shows smaller deflection increments with increase of load:

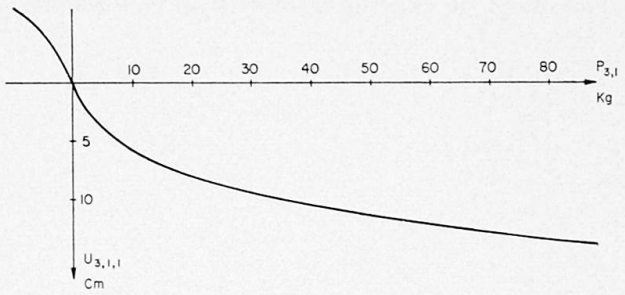

Fig. 11. Curve of $U_{3,1,1}$ versus $P_{3,1}$. $U_{3,1,1}$ means deflection in X_3 (vertical) direction, force application and observation at point 1. Same refers to P.

---

[1]) The first subscript refers to direction, i. e. X_3 or Z axis; the second to the point of application.

under high loads the deflection curve becomes less and less steep and tends to a straight line. This behaviour (common to all displacements and all directions) is due to the load resistance being a combination of a change in shape (referred to later as "bending") and variation of tension in the cables. If small loads act on a plane net, most of the resistance takes the form of "bending"; and the difference in length between the straight and the slightly bent wire being negligible, the variation of tension is also negligible. In a three-dimensional net the situation is different, and variation of tension takes place even with the smallest load. This composite behaviour is the reason for the non-linearity of the graphs. However, as the load increases the net tends to the "funicular" of the applied loads, and further loading of the same mode will no longer cause "bending", except as permitted by the strain in the cables. At this stage additional load may be directly resolved into its components in the net. The non-linearity is of the same order as in an ordinary truss, and deflections are relatively small. The deflection increments at this stage are almost independent of the initial pretension, in contrast to the case of small loads, as explained before (see Fig. 6). In other words: the curve will have the same general shape whatever the rigidity of the cables or the pretension forces. However, for higher rigidities, the slope of the asymptote to the curve will be smaller. In the hypothetical case of $EA = \infty$ the asymptote will be horizontal, since the deflections cannot continue to grow after a certain "bending" level of the net has been reached. If the prestress is increased, the range of transition or non-linear behaviour will increase (Fig. 12). It is of interest that the graph in Fig. 11 is not antisymmetrical, and that deflections are larger for negative loads. This is due to the fact for positive load at point 1, the slope of section 0 increases, while

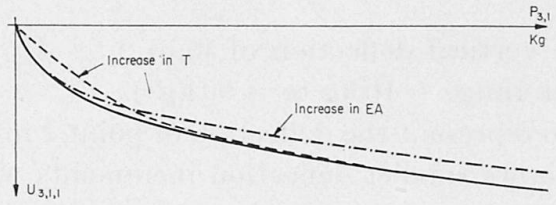

Fig. 12. The effect of varying T or EA on the deflection curve.

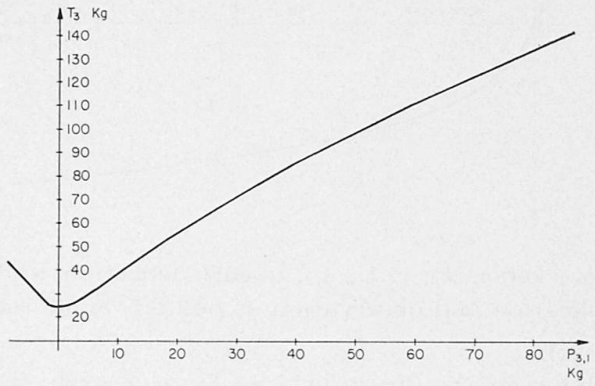

Fig. 13. Curve of T_3 versus $P_{3,1}$.

that of sections 3 and 7 tends to the horizontal. The vertical component in section 0 is the dominant reaction to the load. For negative loads, the slope of section 0 tends to the horizontal, and most of the load is transmitted to anchorage 15. As the distance 1—15 exceeds 1—12, the deflections under negative loads are larger.

A study of T_3 (variation of tension in section 3) versus the load at joint 1 (Fig. 13) shows that it increases for both nagetive and positive loads. The slope of the curve is steeper for negative loads, since for that case the slope of section 3 increases, and the load is transmitted through it to point 15. Fig. 14 shows a blow-up of the curve in the neighborhood of zero load. Minimum tension is obtained at $+0.4$ kg. Near this point variation of tension is small, and the dominant resistance to the load is by "bending". This is why the curve in Fig. 11 is linear and of maximum slope in this interval. This may only be regarded as a general trend, since not all sections have minimum tension simultaneously.

Close inspection of Fig. 13 shows that for high loads the curve is convex while for small loads it is concave. The inflexion point is at about the 8 kg level. The reason for the convexity is that EA is finite, the net continues to deflect, and the change in geometry reduces the deflection increments.

Another interesting curve is that of the vertical deflection of point 3 versus the vertical load at joint 1 (Fig. 15). The curve shows a small negative deflection with a minimum, beyond which the slope becomes positive; above the 77 kg level it deflects beyond its original position. (Note that this graph is drawn on a bigger scale for deflections.)

This behaviour is attributable to the mutually opposite deflections of joints

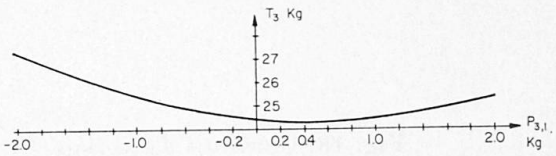

Fig. 14. Blowup of curve 13 near zero load.

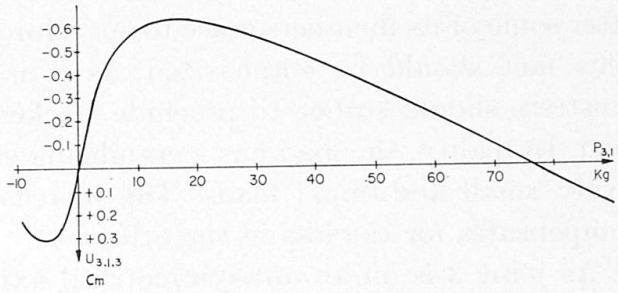

Fig. 15. Curve of $U_{3,1,3}$ versus $P_{3,1}$.

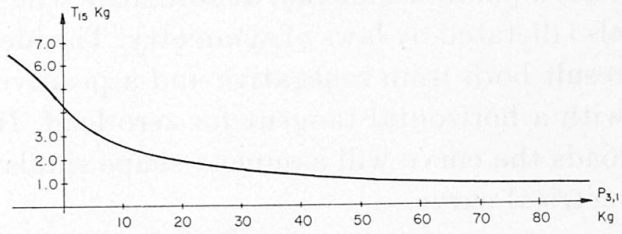

Fig. 16. Curve of T_{15} versus $P_{3,1}$.

3 and 1 under small loads. As the load increases the geometry of the system changes, and joint 1 becomes lower than 3 and pulls down the latter.

The next curve (Fig. 16) shows section 15 which tends to least tension under vertical loading of joint 1. Complete elimination was not observed anywhere.

Loading of Joint 2

As already mentioned, this loading is identical with negative loading of 1.

Loading of Joint 3

Essentially, most of the graphs resemble those shown earlier. However, for this loading, negative tension was obtained in section 2 at 7.25 kg. Fig. 17 shows the deflection of joint 3 under loads up to 15 kg. A dotted line from the load of 7.25 kg shows the theoretical deflection, had the section 2 been capable of withstanding compression. This graph shows that the system is stable even

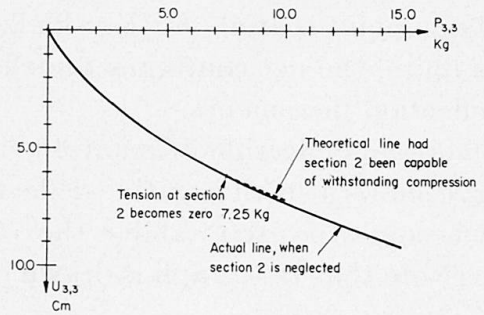

Fig. 17. Curve of $U_{3,3,3}$ versus $P_{3,3}$.

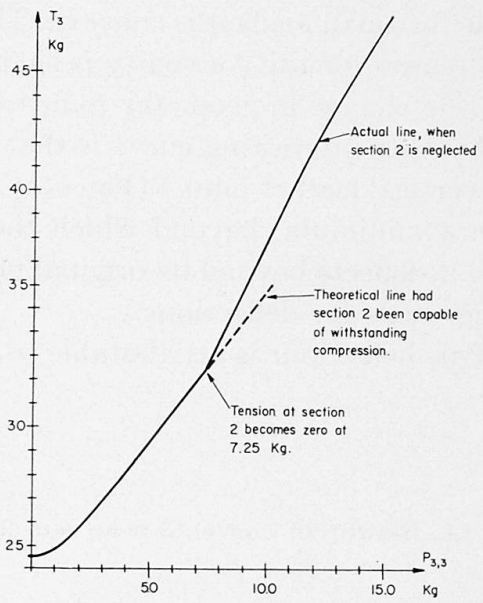

Fig. 18. Curve of T_3 versus $P_{3,3}$.

after some of its members cease to act. Moreover, the discontinuity is negligible. This fact should be emphasized, as it is common practice to believe that prestress should suffice to preclude slackening of the cables under maximum load. In reality, the load has a stabilizing effect on the net with regard to relatively small additional loads. The increased tension in part of the sections compensates for the loss in the others.

As joint 3 is on an antisymmetrical axis, the curve is also antisymmetric, with a point of inflexion at zero load. The tension curve in section 3 (Fig. 18) is also dictated by laws of symmetry. The identical variation of the tension should result both from a negative and a positive load, hence the curve is symmetric with a horizontal tangent for zero load. It should be expected that for higher loads the curve will assume a shape similar to that in Fig. 12, but with a symmetrical curve.

Conclusions

A suspended net may be analyzed by the aid of a computer for any mode of loading, with non-linearity and neutralization of the cables taken into account. The study has shown good agreement between theory and experiment. Lower deflections may be obtained for small concentrated loads by increasing the prestressing forces, and for higher loads by increasing cable rigidity. Deformation of the net may be studied by computer at all stages of construction, and the optimum sequence of applying the roofing may be established. Deformation under the worst combination of suction and pressure wind forces may also be determined. The solution is exact, the only assumption being a weightless net with no moments in the cables. The worked examples have shown that the general method converges rapidly, and is an excellent tool for solving prestressed nets.

The same iterative solution, with a new geometry each time, may be applied to any non-linear problem, including buckling. In the latter case, the denominator determinant must be determined each time. Buckling sets in when determinant vanishes.

Acknowledgements

The experimental part was carried out by U. Etzioni within the framework of an M. Sc. study under the supervision of the author. Y. Partom helped in programming. The project was financed by the Technion — Israel Institute of Technology, Haifa.

Bibliography

1. F. K. Schleyer: Über die Berechnung von Seilnetzen. Dr.-Ing.-Dissertation, Technische Universität Berlin, 1960.
2. F. K. Schleyer: Die Berechnung von Seilnetzen. Colloquium on Hanging Roofs, Continuous Metallic Shell Roofs and Superficial Lattice Roofs, Paris, July 9–11, 1962.
3. A. Siev: Stability of Prestressed Suspended Roofs. D. Sc. thesis, Technion-Israel Institute of Technology, Haifa, 1961.
4. A. Siev: A General Analysis of Prestressed Nets. Publications, International Association for Bridge and Structural Engineering, Vol. 23, page 283, Zurich, 1963.
5. D. N. de G. Allen: Relaxation Methods. McGraw-Hill, 1954. (Formulas on page 31.)
6. A. Siev, J. Eidelman: Stress Analysis of Prestressed Suspended Roofs. Journal of the Structural Engineering Division, A.S.C.E., Vol. 90, No. St. 4, August, 1964.
7. U. Etzioni: Prestressed Suspended Roofs Bounded by Cables. M. Sc. thesis, Technion-Israel Institute of Technology, Haifa, June, 1964. (In Hebrew, with English synopsis.)

Summary

A simple model of a hypar net bounded by parabolic cables was tested under load, one point at a time, up to 2.0 kg in 200 g increments. Discrepancies between theoretically identical deflections were negligible, and no significant hysteresis effects were observed.

A solution obtained by computer was in close agreement. The program was also utilized for higher single loads (including a case of a wire section under zero tension) and for vertical and horizontal loads resp. at all joints.

The study proves the effectiveness and possibilities of computer solution of non-linear problems.

Résumé

Un modèle, simple, de réseau en paraboloïde hyperbolique limité par des câbles paraboliques a été éprouvé sous une charge appliquée séparément à chaque nœud et atteignant progressivement 2,0 kg par augmentations successives de 200 g. Les différences entre les déformations données comme identiques par la théorie se sont révélées négligeables, et l'on n'a pas observé d'effet d'hystérésis significatif.

Une solution a été obtenue en utilisant un ordinateur, et celle-ci est en étroite concordance avec les autres résultats. Le programme mis en œuvre à cet effet a également été appliqué au cas de charges individuelles plus élevées (y compris celui d'un fil supportant une tension nulle) et de charges verticales et horizontales respectivement appliquées à tous les nœuds.

Cette étude met en lumière l'efficacité et les possibilités de l'ordinateur pour la résolution des problèmes non linéaires.

Zusammenfassung

Das untersuchte Modell stellt ein Hyperboloid-Kabeldach dar. Es besteht aus einem Netz sich rechtwinklig kreuzender Drähte, das durch Randdrähte parabolisch begrenzt ist. Jeder Kreuzungspunkt wurde bis zu 2,0 kg belastet mit jeweiligen Laststeigerungen von 200 g. Die gemessenen vertikalen Durchbiegungen zeigen gegenüber den entsprechenden theoretisch ermittelten Werten vernachlässigbar kleine Abweichungen. Hysteresiserscheinungen wurden nicht festgestellt. Die gemessenen Werte sind auch in guter Übereinstimmung mit den Ergebnissen einer Computerberechnung. Das Computerprogramm wurde ferner für höhere Einzelbelastungen (einschließlich eines Falles mit spannungslosem Drahtquerschnitt) und für vertikale und horizontale Lasten benutzt. Dieser Beitrag zeigt die Möglichkeit der Behandlung nichtlinearer Probleme mit Hilfe von Computern.